



In-silico Study for African Plants with Possible Beta-Cell Regeneration Effect through Inhibition of DYRK1A

Ifedibalu Chukwu EIM^{1*}, Chikodili IM², Chikodi EC¹, Ibe CI¹ and Chinenye NH¹

¹Department of Pharmacognosy and Traditional Medicine, Nnamdi Azikiwe University, Nigeria

²Pharmacy Department, National Orthopaedic Hospital, Enugu, Nigeria

***Corresponding author:** Ejiofor InnocentMary IfedibaluChukwu, Department of Pharmacognosy and Traditional Medicine, Faculty of Pharmaceutical Sciences, Nnamdi Azikiwe University, Awka, Anambra State, Nigeria; Email: ii.ejiofor@unizik.edu.ng

Review Article

Volume 6 Issue 3

Received Date: April 22, 2022

Published Date: July 15, 2022

DOI: 10.23880/oajpr-16000270

Abstract

Background: The continuous destruction of normal insulin-producing pancreatic beta cells is a contributing factor in all common forms of diabetes, due to insufficient production of insulin, especially in type 1 diabetes. There are attempts to beta-cells transplantation, but the cost and availability of donors pose a great challenge to the process. Dual-Specificity Tyrosine Phosphorylation-Regulated Kinase A plays a crucial role in beta-cells destruction.

Aims: Our research targets to identify plants for that can be utilized possible alternative approach of beta-cell replacement through a pharmacologically induced regeneration of new beta cells in-silico.

Methods and Material: The 3D structure Dual-Specificity Tyrosine Phosphorylation-Regulated Kinase A and 6511 phytochemicals were obtained from Protein Databank and African Natural Products Database respectively. They were appropriately prepared for molecular docking simulations. Molecular docking simulations were implemented, after validation of docking protocols, in AutoDock-Vina®, using virtual screening scripts. Phytocompounds with good binding affinities for Dual-Specificity Tyrosine Phosphorylation-Regulated Kinase A were selected as frontrunners. The compounds were screened for toxicity and Lipinski's rule confirmation using Datawarrior and then kinase inhibitory bioactivity prediction using Molinspiration.

Results: Twelve phytocompounds were found to be predictably highly active in-silico against Dual-Specificity Tyrosine Phosphorylation-Regulated Kinase A, druglike based on Lipinski's rule, non-mutagenic, non-tumorigenic, no reproductive effect and non-irritant, with high bioactivity prediction.

Conclusions: In-silico active phytocompounds against Dual-Specificity Tyrosine Phosphorylation-Regulated Kinase A with their plant sources and physicochemical parameters were identified. Further studies will be carried out in-vitro and in-vivo in to validate the results of this study using plants containing the identified phytocompounds.

Keywords: Beta-cells; Regeneration; Phytocompounds; DYRK1A; Virtual; Screening; Diabetes

Abbreviations: DYRK1A: Dual-specificity Tyrosine Phosphorylation-regulated Kinase A; PDB: Protein Data Bank; TPSA: Topological Polar Surface Area; RTECS: Registry of Toxic Effects of Chemical Substances; %ABS: Percentage Absorption; DDIG: Drug Design and Informatics Group.

Introduction

Diabetes is a life-threatening global health issue due to its high incidence [1] and associated disability and mortality [2]. The pancreatic beta-cell deficit is a significant component of the pathophysiological mechanism [3]. Beta cells substantial damage results in long-lasting endocrine insufficiency and a permanent diabetic state. Pancreatic beta-cells regeneration is a promising pharmacological strategy for recovering β cells. In adults, it is known that the endocrine pancreas has a regulated ability to regenerate [4]. Consequently, approaches for stimulating beta-cell restoration have insightful inferences for the treatment of diabetes, particularly for type 1 diabetes and late-type two diabetes with considerable beta-cell loss.

There are two approaches through which Pancreatic beta-cells can be regenerated. The first approach is by preventing beta-cell loss precisely through the inhibition of beta-cell apoptosis/necrosis and dedifferentiation. The second approach is to stimulate new endogenous regeneration and exogenous supplementation. For about a century, researchers have attempted pancreatic beta-cells regeneration. Under specific physiological environments, such as pregnancy, obesity, and conditions of insulin resistance, the adaption of islet and improved beta-cell mass take place in both animal models and humans [5-8]. Contemporary advances in new technologies have offered additional substantiation on the generation of beta-cells. Single-cell RNA sequencing data have revealed that human islets comprise four discrete subtypes of beta-cells [9] and potentially transitional stages [10]. These suggest that beta-cells can acclimatize and undergo transdifferentiation or neogenesis. Physiological restoration research can make available data on the development of medication targeted towards beta-cell regeneration. Several approaches have been reported to be utilized in the promotion of beta-cells regeneration. The strategies include pancreatectomy, partial duct ligation, and chemical-induced massive beta-cell loss [11-15]. Molecular routes that cause multiplications in the mass of beta-cells have been comprehensively explored. Thousands of materials have been researched, and hundreds have been demonstrated to be efficient in the course of β cell restoration, but only a small amount is clinical, pre-clinical, or clinical potential medication.

Dual-specificity tyrosine phosphorylation-regulated kinase A (DYRK1A) belongs to the CMGC (CDK, MAPK, CDC-like kinases, GSK3 kinase) family of eukaryotic protein

kinases that have been shown to play essential roles in neurodegenerative diseases [16,17] tumorigenesis and apoptosis [18,19]. More recently, DYRK1A was identified as a regulator of regenerative pathways relevant to human insulin-producing pancreatic β -cells [20-23]. Numerous studies have explored the development of DYRK1A inhibitor scaffolds, given the involvement of DYRK1A in these diseases [17-20,22-24]. Several DYRK1A inhibitors from natural sources like Harmine and small molecule drug discovery programs have been identified and characterized [22,25-48]. Among all the DYRK1A inhibitors, Harmine and its analogues (β -carbolines) are the most commonly studied and remain among the most potent and orally bioavailable classes of inhibitors known [17,49]. Harmine has been proposed to be a hallucinogen due to its presence in the hallucinogenic infusion ayahuasca and its affinity for serotonin, tryptamine, and other receptors in the central nervous system; in addition to its kinase inhibitory effect (CNS) [50,51]. Harmine and its analogues have also been discovered to block DYRK1A-mediated phosphorylation of tau proteins in the CNS [52] and to have anti-proliferative cancer action, including inhibition of topoisomerase I [53,54] inhibition of CDKs [55], activation of cell apoptosis [56], and DNA intercalation [57].

The goals of this research were to determine druggable essential enzyme/target/receptor vital in the pathogenesis of beta-cell apoptosis, identify phytochemicals with high binding affinity against the identified target using molecular docking simulation, determine drug-likeness of these phytochemicals based on Lipinski's rule, determine the toxicity of the phytochemicals in-silico, and undertake bioactivity prediction of the phytochemicals on Molinspiration platform.

Materials and Methods

Materials

Personal computer, African Natural Compounds Database, PubChem (<http://Pubchem.ncbi.nlm.nih.gov>) [58], Linux operating system (Ubuntu desktop 18.04), Protein data bank (<https://www.rcsb.org/>) [59], DataWarrior [60], PyMol [61], AutoDockTools-1.5.6 [62], Autodockvina 1.1.2 [63], on Ubuntu operating system, Molinspiration (<https://www.molinspiration.com/cgi-bin/properties>) [64].

Literature Mining

Literature was mined to identify the target/receptor for possible induction of beta-cell regeneration. This was done to check the importance of the target/receptors in the onset and pathophysiology of destruction. This gives more information about the receptor, functions, properties and its druggability.

Selection and Preparation of the Receptors

After the identification of several target/receptor, literature mining and analysis of the target/receptor, Dual-specificity tyrosine phosphorylation-regulated kinase A in 3D format was obtained from Protein Data Bank with the respective Protein Data Bank (PDB) code; 6UWY. The initial preparation of the pdb file to select the needed chains, delete multiple ligands and non-protein parts was done using PyMol. The PyMol tool was employed to gain insight into the ligands binding to the receptors. The receptor was prepared for molecular docking simulations using AutoDockTool. In the preparation, polar hydrogens and Kollman's charges were added to the receptors and they were saved in pdbqt file format. Pdbqt file format is the structural format needed for the protein and ligand to be in before carrying out the molecular docking simulation. The electrostatic Grid boxes and 3-dimensional affinity of different sizes and centers, as indicated in Table 1 below were created around the active site of the protein.

	6UWY	
	Centres	Sizes
X	-59.224	10
Y	-24.052	8
Z	24.659	12

Table 1: Grid box parameters used for the molecular docking simulations.

Selection, Drug-Likeness and Toxicity Assessment of Ligands (Phytocompounds)

A total number of 6511 phytocompounds isolated were obtained from African Natural Products Database (african-compounds.org) [65,66] in SDF-3D format. The phytocompounds were loaded on to DataWarrior application. Molecular properties such as molecular weight, hydrogen bond donor, hydrogen bond acceptor partition coefficient (Log P), and Topological polar surface area (TPSA) were calculated. Violations of Lipinski's rule of five were observed. The phytocompounds were also screened for toxicity (mutagenicity, carcinogenicity, tumorigenicity and reproductive effect) on the DataWarrior application.

Selection and Preparation of Ligands

Phytocompounds with no violation of Lipinski's rule and no toxicity in-silico were prepared for molecular docking simulation. Reference ligands were identified from the literature and also compound Co-crystallized with the receptor/protein on Protein Data Bank. In preparation of the ligands for molecular docking simulation, all rotatable

bonds, Torsions and Geistesgers charges were assigned and saved as pdbqt files.

Validation of Docking Protocol

In order to validate the molecular docking simulations protocol for the 6UWY (Dual-specificity tyrosine phosphorylation-regulated kinase A) protein, the PDB structure of this protein in complex with a reference inhibitor was reproduced in-silico. The deletion of the reference compound from the protein was done using PyMol. Polar hydrogen, Kollman charges, grid box sizes and centers at a grid space of 1.0 Å were determined with AutoDockTools-1.5.6 [62,63]. The protein was saved in pdbqt file format. The reference compound was prepared for molecular docking simulation using AutoDockTools-1.5.6. Torsions and all rotatable bonds were allowed to stay rotatable. Output was then generated as a pdbqt file extension. Molecular docking simulation of the protein and reference compound was implemented locally using AutoDockVina® [63] on a Linux platform using the centers and sizes with a virtual screening shell script. Docked conformations were visualized in PyMol-1.4.1 and poses were compared with the experimental crystal structures of the reference compound.

Molecular Docking of the Phytocompounds on Dual-Specificity Tyrosine Phosphorylation-Regulated Kinase A

The Phytocompounds were batched for molecular docking simulations against Dual-specificity tyrosine phosphorylation-regulated kinase A, using virtual screening scripts. Molecular docking simulations were carried out in four replicates on a Linux platform using AutoDockVina® and associated tools after validation of docking protocols. Binding free energy values (kcal/mol ± SD) were ranked in order to identify the frontrunner phytocompounds.

Bioactivity Prediction of Phytocompounds

SMILES notations of the frontrunner phytocompounds were fed in the online Molinspiration software version 2011.06 (www.molinspiration.com) to predict bioactivity score for kinase inhibition drug targets.

Calculation of the Predicted Percentage of Absorption

The predicted percentage of absorption (% ab) of the frontrunner phytocompounds were calculated using the method reported by zhao, et al. (2002) [67] by using the following formula: %ab = 109 - (0.345 x TPSA).

Results

Drug-Likeness and Toxicity Assessment of Ligands (Phytochemicals)

The drug-likeness assessment of the 6511 phytochemicals based on Lipinski's rule of five was done to screen out phytochemicals with violations of the rules. After the screening, a total number of 3814 phytochemicals had no violation of Lipinski's rule, while 2697 phytochemicals violated the rules. The 3814 Phytochemicals with no Lipinski's rule violation were subjected to toxicity assessment using Data warrior, to filter out compounds with either mutagenic, tumorigenic, irritant, or reproductive effects. A total number of 1897 phytochemicals were found to have none of the listed toxicities in-silico. Total polar surface area (TPSA) was also analyzed.

Validation of Docking Protocol

The docking protocol validation was done to ensure in-silico reproducibility of the experimental protein-ligand interactions obtained from protein data bank. The results obtained from the docking validations are presented below in Figures 1 and 2 below. Figure 1 represents structural conformation and superimposition of the docked ligand

(blue) and co-crystallized ligand (green) in the Dual-specificity tyrosine phosphorylation-regulated kinase A binding site. Figure 2a shows 2D representation of the co-crystallized ligand-protein interaction, while figure 2b shows 2D representation of the docked ligand-protein interaction. Comparative analysis of the docked ligand and co-crystallized ligand-protein interaction reveals 90.9% match.

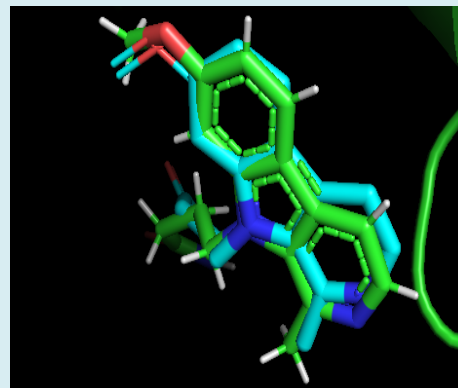


Figure 1: Superimposed view of DYKR1A reference compound in blue and docked reference compound in green.

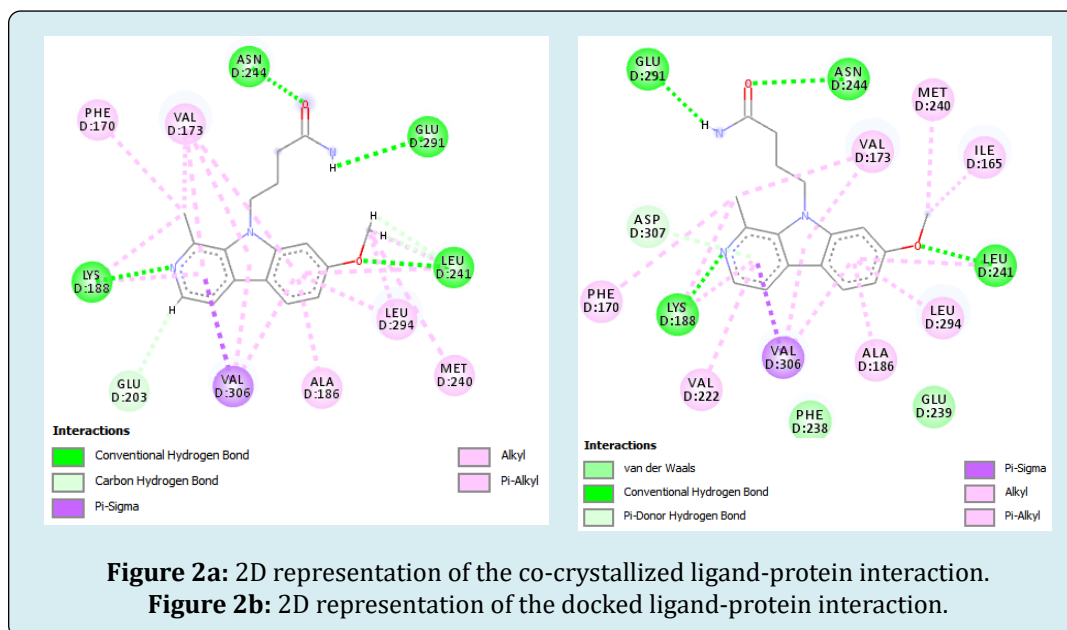


Figure 2a: 2D representation of the co-crystallized ligand-protein interaction.

Figure 2b: 2D representation of the docked ligand-protein interaction.

Molecular Docking of the Phytochemicals DYKR1A Protein

The molecular docking of the phytochemicals was performed on DYKR1A in order to identify phytochemicals with better in-silico inhibitory activity against DYKR1A than the reference compounds. The reference compounds

(highlighted in red) are listed in Table 2. The docking was also performed to study the phytochemicals-proteins interaction pattern at the binding sites of these proteins. Phytochemicals with better binding affinities/energies than the reference compounds (highlighted in red) as can be observed from the mean binding affinity, are presented in Table 2.

S/N	Compound Name	Mean binding affinity	Molecular Weight	cLogP	Hydrogen Acceptor	Hydrogen Donor	TPSA
1	lanuginosine	-11.3 ± 0	305.29	3.46	5	0	57.65
2	4beta,8alpha-dihydroxy-6alpha-vanilloxyloxydauc-9-ene	-11.23 ± 0.06	400.51	3.25	5	1	72.83
3	aegyptinone A	-10.87 ± 0.06	310.39	1.29	3	0	57.2
4	sigmoidin A	-10.70 ± 0.17	424.49	5.86	6	4	107.2
5	penilactone	-10.70 ± 0.00	304.3	1.67	6	1	89.9
6	altertoxin I	-10.60 ± 0.00	352.34	2.36	6	4	115.1
7	sigmoidin B	-10.50 ± 0.00	356.37	3.83	6	4	107.2
8	6,7-dehydro-19beta-hydroxyschizozygin	-10.50 ± 0.00	337.4	0.53	5	1	43.21
9	ungeremine	-10.40 ± 0.00	265.27	3.42	4	1	43.62
10	anastatin B	-10.40 ± 0.00	378.34	3.58	7	4	120.4
11	latrunculin B	-10.40 ± 0.00	357.56	4.49	4	2	83.86
12	Scalarolide	-10.40 ± 0.00	386.57	4.51	3	1	46.53
13	Feselol	-10.40 ± 0.00	386.53	3.61	4	1	55.76
14	assafoetidnol A	-10.40 ± 0.00	398.5	3.15	5	2	75.99
15	chamanetin	-10.40 ± 0.00	364.4	3.8	5	3	86.99
16	neoclerodan-5,10-en-19,6beta,20,12-diolide	-10.40 ± 0.00	315.48	1.96	2	0	40.13
17	chrysophanol- isophyscion bianthrone	-10.37 ± 0.06	508.53	4.63	7	4	124.3
18	3-taraxasterol	-10.30 ± 0.00	430.76	9.48	1	1	20.23
19	helioscopinolide C	-10.30 ± 0.00	330.42	2.43	4	1	63.6
20	3beta-hydroxyisopimaric acid	-10.30 ± 0.00	317.45	1.4	3	1	60.36
21	taraxasterol	-10.23 ± 0.06	424.71	7	1	1	20.23
22	3beta-hydroxymansumbin-13(17)-en-16-one	-10.20 ± 0.00	332.53	4.53	2	1	37.3
23	dihydrofumariline	-10.20 ± 0.00	354.38	1.15	6	2	61.59
24	12alpha-acetoxy-24,25-epoxy-24-hydroxy-20,24-dimethylscalarane	-10.17 ± 0.35	460.7	5.86	4	1	55.76
25	3,4,18-cyclopropa-12-hydroxy-ent-abiet-7-en-16,14-olide	-10.13 ± 0.06	316.44	2.7	3	1	46.53
26	13-hydroxyfeselol	-10.13 ± 0.06	400.51	3.53	5	2	75.99
27	stemmin C	-10.10 ± 0.00	332.48	3.4	3	2	57.53
28	helioscopinolide A	-10.10 ± 0.00	318.46	3.07	3	1	46.53
29	Foetidin	-10.10 ± 0.17	381.49	5.47	4	2	51.83
30	2,11-didehydro-2- dehydroxylycorine	-10.10 ± 0.00	274.34	0.05	4	2	43.13
31	Voucapane	-10.10 ± 0.00	286.46	5.48	1	0	13.14
32	trachyloban-19-oic acid	-10.10 ± 0.00	299.43	1.42	2	0	40.13
33	abyssinin II	-10.10 ± 0.10	370.4	4.11	6	3	96.22
34	(-)-semiglabin	-10.10 ± 0.00	392.41	4.24	6	0	71.06
35	Taraxerone	-10.10 ± 0.61	426.73	7.59	1	0	17.07
36	Pratorinine	-10.07 ± 0.06	267.28	2.63	4	1	49.77
37	Ergosterol	-10.07 ± 0.92	396.66	6.87	1	1	20.23
38	Solanidin	-10.07 ± 0.06	400.67	3.2	2	2	24.67
39	calotropoceryl acetate B	-10.00 ± 0.00	466.75	7.66	2	0	26.3

40	botryorhodine B	-10.00 ± 0.00	314.29	3.45	6	2	93.06
41	asteriscunolide A	-10.00 ± 0.00	250.34	2.93	3	0	43.37
42	diazo derivative of Inuloxin A	-10.00 ± 0.00	264.36	3.61	3	0	35.53
43	Thymelol	-10.00 ± 0.00	354.31	1.87	7	1	91.29
44	Polyanthin	-10.00 ± 0.69	424.54	4.92	5	0	61.83
45	samarcandin	-10.00 ± 0.44	400.51	3.76	5	2	75.99
46	8alpha-isobutanoyloxy-5-alpha-hydroxy-2-oxo-11,13-dehydroguaia-1(10), 3-dien-6alpha,12-olide	-10.00 ± 0.00	334.41	1.85	5	1	72.83
47	aloenin acetal	-10.00 ± 0.00	436.41	0.33	10	3	133.1
48	retroisosenine	-10.00 ± 0.00	336.41	-0.99	6	1	66.27
49	ent-trachyloban-18-oic acid	-10.00 ± 0.00	301.45	1.69	2	0	40.13
50	trachylobane	-10.00 ± 0.00	274.49	5.48	0	0	0
51	lanceolatin B	-10.00 ± 0.00	262.26	3.82	3	0	39.44
52	12-hydroxy-8,12-abietadiene-3,11,14-trione	-10.00 ± 0.00	329.42	1.05	4	0	74.27
53	hosloppone	-10.00 ± 0.00	300.44	4.41	2	2	40.46
54	abyssinone II	-10.00 ± 0.00	324.38	4.52	4	2	66.76
55	lanceolatin A	-9.97 ± 0.40	336.39	4.21	4	1	55.76
56	Postratol	-9.97 ± 0.06	460.61	8.57	4	2	66.76
57	erythroxy-4(17),15(16)-dien-3-one	-9.97 ± 0.06	270.41	4.54	1	0	17.07
58	3-O-benzoylhosloppone	-9.97 ± 0.12	420.55	4.76	4	1	63.6
59	7-keto-8alpha-hydroxy-deepoxysarcophine	-9.93 ± 0.06	332.44	3.49	4	1	63.6
60	3-[6-(3-methyl-but-2-enyl)-1H-indolyl]-6-(3-methyl-but-2-enyl)-1H-indole	-9.93 ± 0.06	368.52	7.25	2	1	20.72
61	(6Z)-cladiellin (cladiella-6Z,11(17)-dien-3-ol)	-9.90 ± 0.00	306.49	4.64	2	1	29.46
62	Hippacine	-9.90 ± 0.00	251.24	2.78	4	2	62.46
63	1,2-dehydrobeninine	-9.90 ± 0.00	327.45	-0.34	4	2	34.93
64	sipholenol J	-9.90 ± 0.00	462.67	4.13	5	3	86.99
65	wtmannin Aor	-9.90 ± 0.00	428.44	1.62	8	0	109.1
66	Gummosin	-9.90 ± 0.00	384.51	3.58	4	1	55.76
67	badrakemin	-9.90 ± 0.35	382.54	4.98	3	2	38.69
68	(-)-samarcondone	-9.90 ± 0.00	398.5	3.78	5	2	72.83
69	Totaradiol	-9.90 ± 0.00	302.46	4.52	2	2	40.46
70	abietatriene	-9.90 ± 0.00	268.44	5.55	0	0	0
71	6,7-dehydroroleanon	-9.90 ± 0.00	313.42	1.48	3	0	57.2
72	5-OH-3-methylnaphtho[2-3-c]furan-4,9-dione	-9.90 ± 0.00	232.23	1.4	4	1	67.51
73	3'-prenylnaringenin	-9.90 ± 0.00	338.36	4.36	5	3	86.99
74	Lysicamine	-9.9 ± 0.	291.31	3.28	4	0	48.42
75	5-deoxyabyssinin II	-9.87 ± 0.15	354.4	4.45	5	2	75.99
76	ekeberin A	-9.87 ± 0.06	456.71	6.19	3	0	35.53
77	aegyptinone B	-9.83 ± 0.06	327.4	1	4	1	77.43
78	pratorimine	-9.8 ± 0	265.27	3.06	4	1	51.46
79	anhydroverlotrin	-9.8 ± 0	250.34	3.09	3	0	43.37

80	nagilactone F	-9.8 ± 0	316.4	2.2	4	0	52.6
81	Totarolone	-9.8 ± 0	300.44	4.66	2	1	37.3
82	voucapan-5-ol	-9.8 ± 0	300.44	4.38	2	1	33.37
83	Coladonin	-9.8 ± 0.82	384.51	3.93	4	1	55.76
84	anhydrolycorine	-9.8 ± 0.17	251.28	2.98	3	0	21.7
85	8-C-p-hydroxybenzyluteolin	-9.8 ± 0.69	392.36	3.56	7	5	124.3
	4-(7-methoxy-1-methyl-9H-beta-carbolin-9-yl)butanamide	-9.80 ± 0.00	297.36	1.97	5	2	70.15
	(1Z)-1-(3-Ethyl-5-hydroxy-2(3H)-benzothiazolylidene)-2-propanone (INDY)	-7.50 ± 0.00	235.31	2.01	3	1	42.23
	GNF4877	-7.28 ± 0.10	494.53	2.51	10	4	143.6

Table 2: Phytocompounds with better binding energy values on DYRK1A than reference compounds.

Bioactivity Prediction of Phytocompounds

Results of the bioactivity prediction of the 85 phytocompounds with better binding affinities than the reference compounds are presented in Table 3. The phytocompounds were screened for kinase inhibitory

activity because the protein of interest; DYRK1A, is a kinase. Twelve phytocompounds were found to possess kinase activity based on the scores. Some of the phytocompounds have better inhibitory scores than the reference compounds as can be observed from Table 3.

S/N	Phytocompounds	Kinase inhibitory	Plant sources
		score	
1	Lysicamine	0.42	<i>Annickia kummeriae</i>
2	lanuginosine	0.4	<i>Magnolia grandiflora</i>
3	Pratorinine	0.4	<i>Crinum americanum</i>
4	Hippacine	0.4	<i>Crinum bulbispermum</i>
5	Pratorimine	0.4	<i>Crinum americanum</i>
6	4-(7-methoxy-1-methyl-9H-beta-carbolin-9-yl)butanamide	0.37	
7	3-[6-(3-methyl-but-2-enyl)-1H-indolyl]-6-(3-methyl-but-2-enyl)-1H-indole	0.32	<i>Monodora angolensis</i>
8	8-C-p-hydroxybenzyluteolin	0.27	<i>Thymus hirtus</i>
9	GNF4877	0.25	
10	3'-prenylnaringenin	0.21	<i>Erythrina abyssinica</i>
11	lanceolatin B	0.15	<i>Tephrosia purpurea</i>
12	lanceolatin A	0.1	<i>Tephrosia purpurea</i>
13	aegyptinone B	0.02	<i>Zhumeria majdae</i>
14	(-)-semiglabin	0	<i>Tephrosia purpurea</i>
15	(1Z)-1-(3-Ethyl-5-hydroxy-2(3H)-benzothiazolylidene)-2-propanone (INDY)	-0.47	

Tables 3: Bioactivity scores of DYRK1A active phytochemicals with their plant sources.

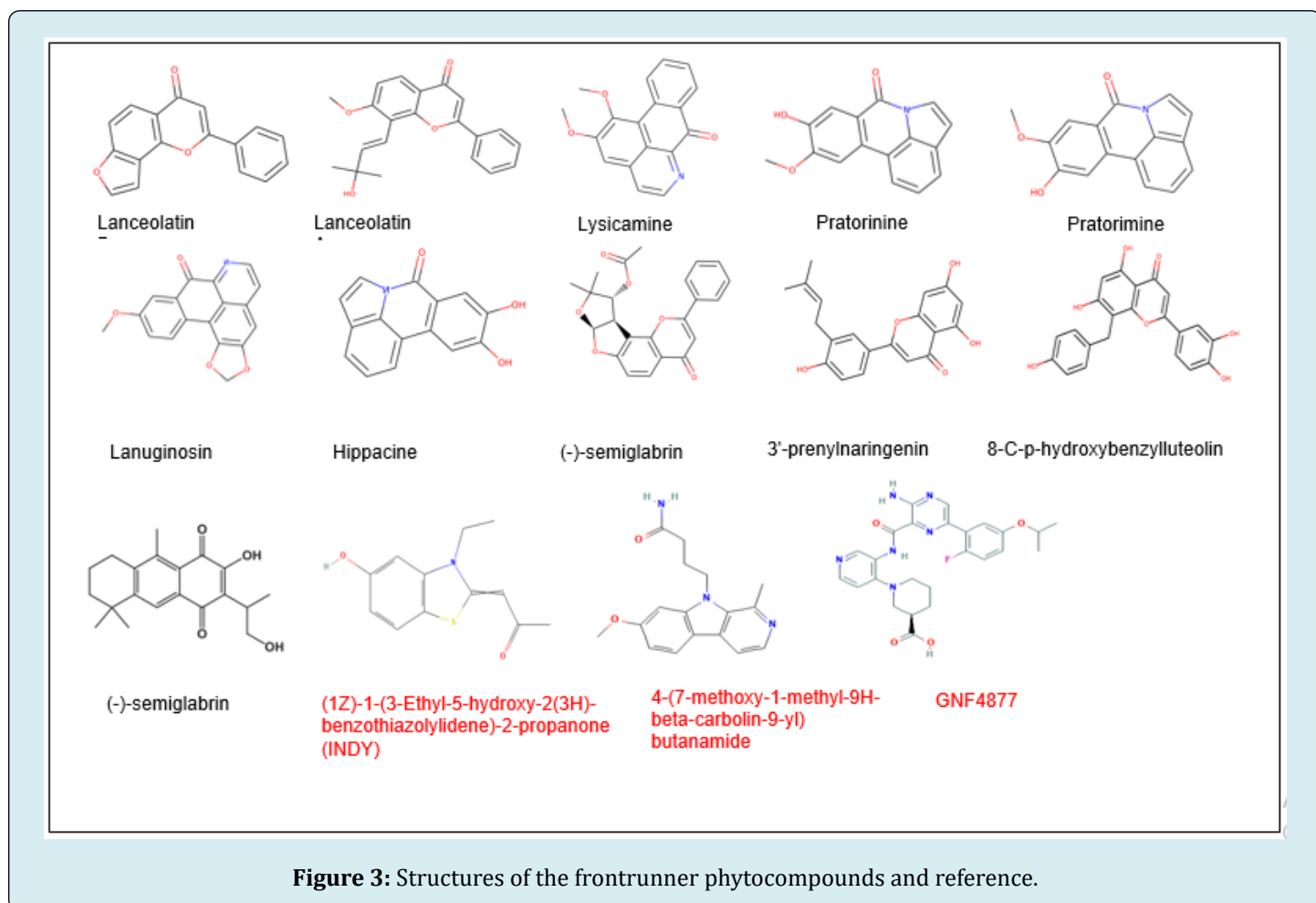
Calculation of the Predicted Percentage of Absorption

The results of the predicted percentage absorption of

the frontrunner phytocompounds with that of the reference compounds are presented in Table 4. The prediction is based on the tPSA values

Compounds	tPSA	%Ab
3-[6-(3-methyl-but-2-enyl)-1H-indolyl]-6-(3-methyl-but-2-enyl)-1H-indole	20.72	101.85
lanceolatin B	39.44	95.39
(1Z)-1-(3-Ethyl-5-hydroxy-2(3H)-benzothiazolylidene)-2-propanone (INDY)	42.23	94.43
Lysicamine	48.42	92.3
Pratorinine	49.77	91.83
Pratorimine	51.46	91.25
lanceolatin A	55.76	89.76
lanuginosine	57.65	89.11
Hippacine	62.46	87.45
4-(7-methoxy-1-methyl-9H-beta-carbolin-9-yl)butanamide	70.15	84.8
(-)-semiglabin	71.06	84.48
aegyptinone B	77.43	82.29
3'-prenylnaringenin	86.99	78.99
8-C-p-hydroxybenzyluteolin	124.29	66.12
GNF4877	143.57	59.47

Table 4: Predicted percentage of absorption.



Discussion

The study set out to determine the binding affinities of phytocompounds from the African natural product database to Dual-specificity tyrosine phosphorylation-regulated kinase A compared to the reference compounds INDY, 4-(7-methoxy-1-methyl-9H-beta-carbolin-9-yl) butanamide and GNF4877 using in silico molecular docking and stimulation. Computer-aided drug design or in-silico approach in drug discovery and design has become an essential tool in modern research. The massive cost of drug discovery and development and the length of time required have made the course of new drug development a challenging one. With components of computer-aided drug design like molecular docking, molecular dynamics, QSAR and ADMET tool and their reliable predictions, drug discovery and development is accelerated. The binding modes between a ligand and a protein can be predicted through molecular docking.

On the other hand, for thousands of ages from early man, medicines and medicinal agents have been sourced from nature, mostly plants. Most medications used today are isolated or developed from isolates obtained from natural sources. Most of these currently used medicines are produced from natural sources based on their use in traditional medicinal practices.

In this study, we obtained 6511 phytocompounds isolated from African plants from the African natural database and first assessed them for drug-likeness using Lipinski's rule of five. Pharmaceutical chemists commonly use Lipinski's rule of five in drug design and development to predict the oral bioavailability of potential lead or drug molecules. According to Lipinski's "rule of five", a candidate molecule will likely be orally active if: a) the molecular weight is below 500, b) the calculated octanol/water partition coefficient (Log P is less than 5, c) the number of hydrogen bond donor is less than five and, d) the number of hydrogen bond acceptor is less than 10 [68-70]. The rule is called "Rule of 5" because the border values are 500 (molecular weight), 5 (clog P), 5 (hydrogen bond donor), and 2*5 (hydrogen bond acceptor).

The in-silico toxicity assessment of the phytocompounds with no violation of Lipinski's rule on the DataWarrior platform relies on a precomputed set of structural fragments that give rise to toxicity alerts if they are encountered in the structures uploaded. These fragment lists were created by rigorously shredding all compounds of the registry of toxic effects of chemical substances (RTECS) database [71] known to be active in a particular toxicity class. During the shredding, compounds were first severed, with each rotating link leading to a set of core fragments. These, in turn, were utilized to reconstitute all possible more significant

components being a substructure of the original molecule. Afterward, a substructure search process determined the occurrence frequency of any fragment (core and constructed fragments) within all compounds of that toxicity class. It also determined these fragment frequencies within the structures of more than 3000 traded drugs. Based on the assumption that sold drugs are primarily free of toxic effects, any fragment was considered a risk factor if it often occurred as the substructure of harmful compounds but never or rarely in traded drugs. Based on this explained fragments search, a total number of 1897 phytocompounds showed no in-silico mutagenicity, tumorigenicity, irritant and reproductive effects. These phytocompounds contain no fragments or fragments known to have any of the toxicities listed according to the registry of toxic effects of chemical substances.

From the molecular docking result, 85 phytocompounds were obtained with better binding affinity than the reference compounds, as shown in table 2. Lower binding affinity suggests better ligand binding. The importance of binding affinity values is determined by the most significant magnitude negative value, representing the most favourable conformation of the complex formed when the ligand involved efficiently binds with the protein's active site. As observed, the mean binding affinity scores are in negative values. This is because protein-ligand binding only occurs spontaneously when the free energy change is negative, and the difference in ΔG levels of complexed and unbound free states is proportional to the stability of the protein-ligand interaction. Both protein folding and protein-ligand binding occur when ΔG is low in the system [72, 73]. Hence, negative ΔG scores indicate the stability of the resulting complexes with receptor molecules, which is an essential characteristic of efficacious drugs [74].

From the molinspiration bioactivity prediction, twelve compounds were found to be very active kinase inhibitors. Based on the prediction, two of the three reference compounds used were also very active kinase inhibitors. One of the reference compounds was predicted to be a moderately active kinase inhibitor. In molinspiration, biological activity is measured by bioactivity score that is categorized as active (0.00 to 0.5), moderately active (0.00 to -0.5), inactive (less than -0.5) [64].

The calculated percentage absorption (%ABS) of the frontrunner phytocompounds ranged between 66.12% and 101.85%, indicating that these phytocompounds have good permeability in the cellular membrane. The percentage absorption was calculated from the topological polar surface area (TPSA). The frontrunner phytocompounds exhibited computational TPSA values between 20.72 and 124.29 Å² and have good intestinal absorption. As a guide, orally active

drugs transported by the transcellular route should not exceed a PSA of about 120 Å² [75,76]. Similarly, for good brain penetration of CNS drugs, this number should even be tailored to PSA < 100 Å² [76] or even smaller, < 60–70 Å² [75].

Finally, observation of the frontrunner phytochemicals' structures compared with reference compounds, as presented in figure 3, reveals some structural activity relationships that might be necessary for the inhibition of DYRK1A. The frontrunner compounds are composed of phenolics and alkaloids. From the 2D structure of the PDB reference compound presented in Figure 2, it can be observed that Nitrogen, Oxygen and Hydrogen atoms are necessary for the protein-ligand interaction, which are all components of the frontrunner phytochemicals. Previous in-vitro research has shown that some natural products, alkaloids, and polyphenolic compounds act as inhibitors of DYRK1A. Polyphenol epigallocatechin gallate, a major catechin component of green Tea, when tested in a panel of 28 kinases structurally and functionally related to DYRK1A, it proved to be selective, showing inhibitory activity only against DYRK1A (IC₅₀ 330 nM [ATP] = 100 μM) [77]. Acaninol B, isolated in 2010 from *Acacia nilotica* [78], a plant of the Leguminosae family, showed moderate activity against DYRK1A (IC₅₀ 19 μM [ATP] = 15 μM) [79]. The screening of a set of natural flavonoids and synthetic flavonoidal alkaloids against a panel of five kinases led to the identification of the already known CDK inhibitor flavopiridol [80,81], as a potent DYRK1A inhibitor (IC₅₀ 0.3 μM) [82]. Staurosporine, an indolecarbazole isolated from *Streptomyces staurosporeus* [83] bearing a sugar moiety bound to both indole nitrogen atoms, is a potent DYRK1A inhibitor (IC₅₀ 19 nM) but highly nonselective toward other kinases [84,85]. Its analogue, bearing an L-rhamnulose moiety, is also significantly active against DYRK1A (IC₅₀ 4 nM) [85,86]. Acrifoline, an alkaloid, has been shown to be a potent DYRK1A inhibitor (IC₅₀ 0.075 μM). Chlorospermine B and Atalaphyllidine are moderately active inhibitors of DYRK1A [87]. Two granulatimide analogues have recently shown potent activity as DYRK1A inhibitors with IC₅₀ values of 0.26 and 0.09 μM, respectively [88,89].

Conclusion

Because options for treating beta cell regeneration are a major unmet therapeutic need, small inhibition of the DYRK1A molecules can provide a solution for pharmaceutical intervention of beta cell regeneration in diabetes. Nonetheless, due to the traditional role of DYRK1A in regulating several signaling pathways critical to neuronal development and functions, its modulation should be sought with caution in order to minimize its activity to the levels normally observed in healthy individuals. The results of this present in-silico experiments suggest that 3-[6-(3-methyl-but-2-enyl)-1H-

indolyl]-6-(3-methyl-but-2-enyl)-1H-indole, lanceolatin B, lysicamine, pratorinine, Pratorimine, lanceolatin A, lanuginosine, Hippacine, (-)-semiglabin, aegyptinone B, 3'-prenylnaringenin and 8-C-p-hydroxybenzyluteolin are candidate ligands for activating beta-cells regeneration. Computational drug-likeness and TPSA and percentage absorption calculations revealed that the phytochemicals show good intestinal absorption. Finally, the in-silico study has identified these phytochemicals as potential new drug candidates. More detailed studies with other models, such as in-vivo assays, with these phytochemicals or extracts containing these phytochemicals, are essential for validating this in-silico study.

Acknowledgment

We express our gratitude to the Principal Investigator, Drug Design and Informatics Group (DDIG) laboratory, for grand us free access to the facility. We appreciate the contribution of the CURIRES research team of the Faculty of Pharmaceutical Sciences, Nnamdi Azikiwe University, Awka to this ongoing research.

References

1. Li Y, Teng D, Shi X, Qin G, Qin Y, et al. (2020) Prevalence of Diabetes Recorded in Mainland China Using 2018 Diagnostic Criteria from the American Diabetes Association: National Cross Sectional Study. *BMJ* 369: m997.
2. Zhou M, Wang H, Zeng X, Yin P, Zhu J, et al. (2019) Mortality, Morbidity, and Risk Factors in China and its Provinces, 1990-2017: A Systematic Analysis for the Global Burden of Disease Study 2017. *Lancet* 394 (10204): 1145-1158.
3. Matveyenko AV, Butler PC (2008) Relationship between Beta-Cell Mass and Diabetes Onset. *Diabetes Obes Metab* 10(4): 23-31.
4. Cnop M, Igoillo-Esteve M, Hughes SJ, Walker JN, Cnop I, et al. (2011) Longevity of Human Islet A- and B-Cells. *Diabetes Obes Metab* 13: 39-46.
5. Rieck S, Kaestner KH (2010) Expansion of Beta-Cell Mass in Response to Pregnancy. *Trends Endocrinol Metab* 21(3): 151-158.
6. Kahn SE, Hull RL, Utzschneider KM (2006) Mechanisms Linking Obesity to Insulin Resistance and Type 2 Diabetes. *Nature* 444(7121): 840-846.
7. Butler AE, Cao-Minh L, Galasso R, Rizza RA, Corradin A, et al. (2010) Adaptive Changes in Pancreatic Beta-Cell Fractional Area and Beta Cell Turnover in Human

- Pregnancy. *Diabetologia* 53(10): 2167-2176.
8. Mezza T, Muscogiuri G, Sorice GP, Clemente G, Hu J, et al. (2014) Insulin Resistance Alters Islet Morphology in Nondiabetic Humans. *Diabetes* 63(3): 994-1007.
 9. Dorrell C, Schug J, Canaday PS, Russ HA, Tarlow BD, et al. (2016) Human Islets Contain Four Distinct Subtypes of B Cells. *Nat Commun* 7: 11756.
 10. Segerstolpe Å, Palasantza A, Eliasson P, Andersson EM, Andréasson AC, et al. (2016) Single-Cell Transcriptome Profiling of Human Pancreatic Islets in Health and Type 2 Diabetes. *Cell Metab* 24(4): 593-607.
 11. Li WC, Rukstalis JM, Nishimura W, Tchipashvili V, Habener JF, et al. (2010) Activation of Pancreatic-Duct-Derived Progenitor Cells During Pancreas Regeneration in Adult Rats. *J Cell Sci* 123: 2792-2802.
 12. Thorel F, Népote V, Avril I, Kohno K, Desgraz R, et al. (2010) Conversion of Adult Pancreatic Alpha-Cells to Beta-Cells After Extreme Beta-Cell Loss. *Nature* 464(7292): 1149-1154.
 13. Chera S, Baronnier D, Ghila L, Cigliola V, Jensen JN, et al. (2014) Diabetes Recovery by Age-Dependent Conversion of Pancreatic δ -Cells Into Insulin Producers. *Nature* 514(7523): 503-507.
 14. Xu X, D'Hoker J, Stangé G, Bonné S, De Leu N, et al. (2008) Beta Cells can be Generated from Endogenous Progenitors in Injured Adult Mouse Pancreas. *Cell* 132(2): 197-207.
 15. Bonner-Weir S, Baxter LA, Schupp GT, Smith FE (1993) A Second Pathway for Regeneration of Adult Exocrine and Endocrine Pancreas. A Possible Recapitulation of Embryonic Development. *Diabetes* 42(12): 1715-1720.
 16. Wegiel J, Gong C-X, Hwang Y-W (2011) The Role of DYRK1A in Neurodegenerative Diseases. *FEBS J* 278(2): 236-245.
 17. Smith B, Medda F, Gokhale V, Dunckley T, Hulme C (2012) Recent Advances in the Design, Synthesis and Biological Evaluation of Selective DYRK1A Inhibitors: A New Avenue for a Disease Modifying Treatment of Alzheimer's? *ACS Chem Neurosci* 3(11): 857-872.
 18. Ionescu A, Dufresne F, Gelbcke M, Jabin I, Kiss R, et al. (2012) DYRK1A Kinase Inhibitors with Emphasis on Cancer. *Mini Rev Med Chem* 12(13): 1315-1329.
 19. Fernandez-Martinez P, Zahonero C, Sanchez-Gomez P (2015) DYRK1A: The Double-Edged Kinase as a Protagonist in Cell Growth and Tumorigenesis. *Mol Cell Oncol* 2(1): e970048.
 20. Wang P, Alvarez-Perez J-C, Felsenfeld DP, Liu H, Sivendran S, et al. (2015) A High-Throughput Chemical Screen Reveals that Harmine-Mediated Inhibition of DYRK1A Increases Human Pancreatic Beta Cell Replication. *Nat Med* 21(4): 383-388.
 21. Shen W, Taylor B, Jin Q, Nguyen-Tran V, Meeusen S, et al. (2015) Inhibition of DYRK1A and GSK3B Induces Human B-Cell Proliferation. *Nat Commun* 6: 8372-8382.
 22. Rachdi L, Kariyawasam D, Aiello V, Herault Y, Janel N, et al. (2014) Dyrk1A Induces Pancreatic B Cell Mass Expansion and Improves Glucose Tolerance. *Cell Cycle* 13(14): 2221-2229.
 23. Dirice E, Walpita D, Vetere A, Meier BC, Kahraman S, et al. (2016) Inhibition of DYRK1A Stimulates Human Beta-Cell Proliferation. *Diabetes* 65(6): 1660-1671.
 24. Becker W, Soppa U, Tejedor FJ (2014) DYRK1A: A Potential Drug Target for Multiple Down Syndrome Neuropathologies. *CNS Neurol Disord Drug Targets* 13(1): 26-33.
 25. Guedj F, Sebric C, Rivals I, Ledru A, Paly E, et al. (2009) Green Tea Polyphenols Rescue of Brain Defects Induced by Overexpression of DYRK1A. *PLoS One* 4(2): e4606.
 26. McLauchlan H, Elliott M, Cohen P (2003) The Specificities of Protein Kinase Inhibitors: An Update. *Biochem J* 371: 199-204.
 27. Tahtouh T, Elkins JM, Filippakopoulos P, Soundararajan M, Burgy G, et al. (2012) Selectivity, Cocrystal Structures, and Neuroprotective Properties of Leucettines, A Family of Protein Kinase Inhibitors Derived from the Marine Sponge Alkaloid Leucettamine B. *J Med Chem* 55(21): 9312-9330.
 28. Naert G, Ferre V, Meunier J, Keller E, Malmstrom S, et al. (2015) Leucettine L41, A DYRK1A-Preferential Dyrks/Clks Inhibitor, Prevents Memory Impairments and Neurotoxicity Induced by Oligomeric A β 25-35 Peptide Administration in Mice. *Eur Neuropsychopharmacol* 25(11): 2170-2182.
 29. Cozza G, Mazzorana M, Papinutto E, Bain J, Elliott M, et al. (2009) Quinalizarin as a Potent, Selective and Cell-Permeable Inhibitor of Protein Kinase CK2. *Biochem J* 421(3): 387-395.
 30. Ahmadu A, Abdulkarim A, Grougnet R, Myriantopoulos V, Tillequin F, et al. (2010) Two New Peltogynoids from *Acacia Nilotica* Delile with Kinase Inhibitory Activity. *Planta Med* 76(5): 458-460.

31. Sarno S, Mazzorana M, Traynor R, Ruzzene M, Cozza G, et al. (2012) Structural Features Underlying the Selectivity of the Kinase Inhibitors NBC and Dnbc: Role of a Nitro Group that Discriminates between CK2 and DYRK1A. *Cell Mol Life Sci* 69(3): 449-460.
32. Sanchez C, Salas AP, Brana AF, Palomino M, Pineda-Lucena A, et al. (2009) Generation of Potent and Selective Kinase Inhibitors by Combinatorial Biosynthesis of Glycosylated Indolocarbazoles. *Chem Commun* 27: 4118-4120.
33. Ogawa Y, Nonaka Y, Goto T, Ohnishi E, Hiramatsu T, et al. (2010) Development of a Novel Selective Inhibitor of the Down Syndrome-Related Kinase Dyrk1A. *Nat Commun* 1: 86.
34. Gourdain S, Dairou J, Denhez C, Bui LC, Rodrigues-Lima F, et al. (2013) Development of Dandys, New 3,5-Diaryl-7-Azaindoles Demonstrating Potent DYRK1A Kinase Inhibitory Activity. *J Med Chem* 56(23): 9569-9585.
35. Kii I, Sumida Y, Goto T, Sonamoto R, Okuno Y, et al. (2016) Selective Inhibition of the Kinase DYRK1A by Targeting its Folding Process. *Nat Commun* 7: 11391-11404.
36. Koo KA, Kim ND, Chon YS, Jung M-S, Lee B-J, et al. (2009) QSAR Analysis of Pyrazolidine-3,5-Diones Derivatives as Dyrk1A Inhibitors. *Bioorg Med Chem Lett* 19(8): 2324-2328.
37. Kim ND, Yoon J, Kim JH, Lee JT, Chon YS, et al. (2006) Putative Therapeutic Agents for the Learning and Memory Deficits of People with Down Syndrome. *Bioorg Med Chem Lett* 16(14): 3772-3776.
38. Rosenthal AS, Tanega C, Shen M, Mott BT, Bougie JM, et al. (2011) Potent and Selective Small Molecule Inhibitors of Specific Isoforms of Cdc2-Like Kinases (Clk) and Dual Specificity Tyrosine-Phosphorylation-Regulated Kinases (Dyrk). *Bioorg Med Chem Lett* 21(10): 3152-3158.
39. Giraud F, Alves G, Debiton E, Nauton L, Thery V, et al. (2011) Synthesis, Protein Kinase Inhibitory Potencies, and *In Vitro* Antiproliferative Activities of Meridianin Derivatives. *J Med Chem* 54(13): 4474-4489.
40. Echalié A, Bettayeb K, Ferandin Y, Lozach O, Clément M, et al. (2008) Meriolins (3-(Pyrimidin-4-yl)-7-Azaindoles): Synthesis, Kinase Inhibitory Activity, Cellular Effects, and Structure of a CDK2/Cyclin A/Meriolin Complex. *J Med Chem* 51(4): 737-751.
41. Akue-Gedu R, Debiton E, Ferandin Y, Meijer L, Prudhomme M, et al. (2009) Synthesis and Biological Activities of Aminopyrimidyl-Indoles Structurally Related to Meridianins. *Bioorg Med Chem* 17(13): 4420-4424.
42. Kassis P, Brzeszcz J, Beneteau V, Lozach O, Meijer L, et al. (2011) Synthesis and Biological Evaluation of New 3-(6-Hydroxyindol-2-yl)-5-(Phenyl) Pyridine or Pyrazine V-Shaped Molecules as Kinase Inhibitors and Cytotoxic Agents. *Eur J Med Chem* 46(11): 5416-5434.
43. Neagoie C, Vedrenne E, Buron F, Merour J-Y, Rosca S, et al. (2012) Synthesis of Chromeno[3,4-B]Indoles as Lamellarin D Analogues: A Novel DYRK1A Inhibitor Class. *Eur J Med Chem* 49: 379-396.
44. Falke H, Chaikuad A, Becker A, Loac N, Lozach O, et al. (2015) 10-Iodo-11H-Indolo[3,2-C]Quinoline-6-Carboxylic Acids are Selective Inhibitors of DYRK1A. *J Med Chem* 58(7): 3131-3143.
45. Foucourt A, Hedou D, Dubouilh-Benard C, Desire L, Casagrande A-S, et al. (2014) Design and Synthesis of Thiazolo[5,4-F]Quinazolines as DYRK1A Inhibitors, Part I. *Molecules* 19(10): 15546-15571.
46. Coutadeur S, Benyamine H, Delalonde L, de Oliveira C, Leblond B, et al. (2015) A Novel DYRK1A (Dual Specificity Tyrosine Phosphorylation-Regulated Kinase 1A) Inhibitor for the Treatment of Alzheimer's Disease: Effect on Tau and Amyloid Pathologies *In Vitro*. *J Neurochem* 133(3): 440-451.
47. Abdolazimi Y, Lee S, Xu H, Allegretti P, Horton TM, et al. (2018) CC-401 Promotes B-Cell Replication Via Pleiotropic Consequences of DYRK1A/B Inhibition. *Endocrinology* 159(9): 3143-3157.
48. Annes JP, Ryu JH, Lam K, Carolan PJ, Utz K, et al. (2012) Adenosine Kinase Inhibition Selectively Promotes Rodent and Porcine Islet β -Cell Replication. *Proc Natl Acad Sci U S A* 109(10): 3915-3920.
49. Becker W, Sippl W (2011) Activation, Regulation, and Inhibition of DYRK1A. *FEBS J* 278(2): 246-256.
50. Brierley DI, Davidson C (2012) Developments in Harmine Pharmacology - Implications for Ayahuasca Use and Drug-Dependence Treatment. *Prog Neuro-Psychopharmacol Biol Psychiatry* 39(2): 263-272.
51. Airaksinen MM, Lecklin A, Saano V, Tuomisto L, Gynther J (1987) Tremorigenic Effect and Inhibition of Tryptamine and Serotonin Receptor Binding by β -Carbolines. *Pharmacol Toxicol* 60(1): 5-8.
52. Frost D, Meechoovet B, Wang T, Gately S, Giorgetti M, et al. (2011) β -Carboline Compounds, Including Harmine, Inhibit DYRK1A and Tau Phosphorylation at Multiple Alzheimer's Disease-Related Sites. *PLoS One* 6(5): 4420-4424.

- e19264.
53. Cao R, Peng W, Chen H, Ma Y, Liu X, et al. (2005) DNA Binding Properties of 9-Substituted Harmine Derivatives. *Biochem Biophys Res Commun* 338(3): 1557-1563.
 54. Sobhani AM, Ebrahimi S-A, Mahmoudian M (2002) An *In Vitro* Evaluation of Human DNA Topoisomerase I Inhibition by Peganum Harmala L. Seeds Extract and Its B-Carboline Alkaloids. *J Pharm Pharm Sci* 5(1): 18-22.
 55. Song Y, Kesuma D, Wang J, Deng Y, Duan J, et al. (2004) Specific Inhibition of Cyclin-Dependent Kinases and Cell Proliferation by Harmine. *Biochem Biophys Res Commun* 317(1): 128-132.
 56. Cao M-R, Li Q, Liu Z-L, Liu H-H, Wang W, et al. (2011) Harmine Induces Apoptosis in Hepg2 Cells Via Mitochondrial Signaling Pathway. *Hepatobiliary Pancreatic Dis Int* 10(6): 599-604.
 57. Taira Z, Kanzawa S, Dohara C, Ishida S, Matsumoto M, et al. (1997) Intercalation of Six β -Carboline Derivatives Into DNA. *Jpn J Toxicol Environ Health* 43(2): 83-91.
 58. Kim S, Chen J, Cheng T, Gindulyte A, He J, et al. (2019) Pubchem in 2021: New Data Content and Improved Web Interfaces. *Nucleic Acids Res* 49: D1388-D1395.
 59. Berman HM, Westbrook J, Feng Z, Gilliland G, Bhat TN, et al. (2000) The Protein Data Bank. *Nucleic Acids Research* 28(1): 235-242.
 60. Sander T, Freyss J, von Korff M, Rufener C (2015) DataWarrior: An Open-Source Program for Chemistry Aware Data Visualization and Analysis. *J Chem Inf Model* 55(2): 460-473.
 61. The PyMOL Molecular Graphics System, Version 1.2r3pre, Schrödinger, LLC.
 62. Sanner MF (1999) Python: A Programming Language for Software Integration and Development. *J Mol Graph Model* 17(1): 57-61.
 63. Trott O, Arthur JO (2009) AutoDock Vina: Improving the Speed and Accuracy of Docking with a New Scoring Function, Efficient Optimization, and Multithreading. *J Comput Chem* 31(2): 455-461.
 64. Molinspiration Cheminformatics. Slovensky Grob, Slovakia.
 65. Simoben CV, Qaseem A, Moumbock AFA, Telukunta KK, Günther S, et al. (2020) Pharmacoinformatic Investigation of Medicinal Plants from East Africa. *Molecular Informatics* 39(11): 2000163.
 66. Ntie-Kang F, Telukunta KK, Döring K, Simoben CV, Moumbock AFA, et al. (2017) NANPDB: A Resource for Natural Products from Northern African Sources. *J Nat Prod* 80(7): 2067-2076.
 67. Zhao YH, Abraham MH, Le J, Hersey A, Luscombe CN, et al. (2002) Rate-Limited Steps of Human Oral Absorption and QSAR Studies. *Pharm Res* 19(10): 1446-1457.
 68. Lipinski CV, Lombardo F, Dominy BW, Feeney PJ (1997) Experimental and Computational Approaches to Estimate Solubility and Permeability in Drug Discovery and Development Settings. *Advanced Drug Delivery Reviews* 23(1-3): 3-25.
 69. Lipinski CV, Lombardo F, Dominy BW, Feeney PJ (2001) Experimental and Computational Approaches to Estimate Solubility and Permeability in Drug Discovery and Development Settings. *Adv Drug Deliv Rev* 46(1-3): 3-26.
 70. Lipinski CA (2004) Lead- and Drug-Like Compounds: The Rule-of-Five Revolution. *Drug Disco Today: Techno* 1(4): 337-341.
 71. BIOVIA Databases | Bioactivity Databases: RTECS. accelrys.com.
 72. Sergeev YV, Dolinska MB, Wingfield PT (2014) Thermodynamic Analysis of Weak Protein Interactions Using Sedimentation Equilibrium. *Curr. Protoc Protein Sci* 77: 1-15.
 73. Du X, Li Y, Xia YL, Ai SM, Liang J, Sang P, et al (2016) Insights into Protein-Ligand Interactions: Mechanisms, Models, and Methods. *Int J Mol Sci* 17(2): 144.
 74. Muthu S, Durairaj B (2016) Molecular Docking Studies on Interaction of Annona Muricata Compounds with Antiapoptotic Proteins Bcl-2 and Surviving. *Sky J Biochem Res* 5(2): 14-17.
 75. Clark DE (1999) Rapid Calculation of Polar Molecular Surface Area and Its Application to the Prediction of Transport Phenomena. 2. Prediction of Blood-Brain Barrier Penetration. *J Pharm Sci* 88(8): 815-821.
 76. Kelder J, Grootenhuys PD, Bayada DM, Delbressine LP, Ploemen JP (1999) Polar Molecular Surface as a Dominating Determinant for Oral Absorption and Brain Penetration of Drugs. *Pharm Res* 16(10): 1514-1519.
 77. De la Torre R, De Sola S, Pons M, Duchon A, de Lagran MM, et al. (2014) Epigallocatechin3-Gallate, A DYRK1A Inhibitor, Rescues Cognitive Deficits in Down Syndrome Mouse Models and in Humans. *Mol Nutr Food Res* 58(2): 278-288.

78. *Acacia nilotica* (acacia) | Plants & Fungi At Kew.
79. Stotani S, Giordanetto F, Medda F (2016) DYRK1A Inhibition as Potential Treatment for Alzheimer's Disease. *Future Medicinal Chemistry* 8(6): 681-696.
80. Kelland LR (2000) Flavopiridol, the First Cyclin-Dependent Kinase Inhibitor to Enter the Clinic: Current Status. *Expert Opin Investig Drugs* 9(12): 2903-2911.
81. Raje N, Hideshima T, Mukherjee S, Raab M, Vallet S, et al. (2009) Preclinical Activity of P276-00, A Novel Small-Molecule Cyclin-Dependent Kinase Inhibitor in the Therapy of Multiple Myeloma. *Leukemia* 23(5): 961-970.
82. Nguyen TB, Lozach O, Surpateanu G, Wang Q, Retailleau P, et al. (2012) Synthesis, Biological Evaluation, and Molecular Modeling of Natural and Unnatural Flavonoidal Alkaloids, Inhibitors of Kinases. *J Med Chem* 55(6): 2811-2819.
83. Omura S, Iwai Y, Hirano A, Nakagawa A, Awaya J, et al. (1977) A New Alkaloid AM-2282 OF *Streptomyces* Origin. Taxonomy, Fermentation, Isolation and Preliminary Characterization. *J Antibiot (Tokyo)* 30(4): 275-282.
84. Rüegg UT, Gillian B (1989) Staurosporine, K-252 and UCN-01: Potent but Nonspecific Inhibitors of Protein Kinases. *Trends Pharmacol Sci* 10(6): 218-220.
85. Sánchez C, Salas AP, Braña AF, Palomino M, Pineda-Lucena A, et al. (2009) Generation of Potent and Selective Kinase Inhibitors by Combinatorial Biosynthesis of Glycosylated Indolocarbazoles. *Chem Commun* 27: 4118-4120.
86. Genilloud O, Vicente F, Thurston DE (2012) Drug Discovery from Natural Products. Royal Society of Chemistry, Granada, Spain.
87. Beniddir MA, Le Borgne E, Iorga BI, Loaëc N, Lozach O, et al. (2014) Acridone Alkaloids from *Glycosmis Chlorosperma* as DYRK1A Inhibitors. *J Nat Prod* 77(5): 1117-1122.
88. Deslandes S, Chassaing S, Delfourne E (2010) Synthesis of Two Series of Pyrazolic Analogs of the Marine Alkaloids Granulatimide and Isogranulatimide as Potent Checkpoint 1 Kinase Inhibitors. *Tetrahedron Letters* 51(43): 5640-5642.
89. Deslandes S, Lamoral-Theys D, Frongia C, Chassaing S, Bruyère C, et al. (2012) Synthesis and Biological Evaluation of Analogs of the Marine Alkaloids Granulatimide and Isogranulatimide. *Eur J Med Chem* 54: 626-636.

